Fabrication of UV detectors based on ZnO nanowires using silicon microchannel

J.P. Kar [a], S.N. Das [a], J.H. Choi [a], Y.A. Lee [b], T.Y. Lee [b], J.M. Myoung [a],*

[a] *Information and Electronic Materials Research Laboratory, Department of Materials Science and Engineering, Yonsei University, 134 Shinchon-Dong, Seoul 120-749, Republic of Korea*
[b] *Nanobio Fusion Device Laboratory, Department of Electrical and Electronic Engineering, Yonsei University, 134 Shinchon-Dong, Seoul 120-749, Republic of Korea*

ARTICLE INFO

ABSTRACT

Aligned ZnO nanowires were grown by metal organic chemical vapor deposition on patterned silicon substrate. The shape of nanostructures was greatly influenced by the micropatterned surface. The aspect ratio, packing fraction and the number density of nanowires on top surface are around 10, 0.8 and 10^7 per mm^2, respectively, whereas the values are 20, 0.3 and 5×10^7 per mm^2, respectively, towards the bottom of the cavity. XRD patterns suggest that the nanostructures have good crystallinity. High-resolution transmission electron microscopy confirmed the single-crystalline growth of the ZnO nanowires along the [0 0 0 1] direction. Photosensitivity of the nanowires, grown on both top and bottom surface of the microchannel, was observed. However, the nanowires grown on bottom surface have shown better UV response with base line recovery at dark condition.

© 2009 Elsevier B.V. All rights reserved.

1. Introduction

In recent years, ZnO nanowires have drawn considerable attentions for fundamental studies and applications as building blocks of various nanoscale devices [1,2]. As a wide bandgap semiconductor, there has been promising progress in the bandgap engineering of ZnO. The energy bandgap is tunable from 2.8 to 3.3 eV and 3.3 to 4 eV by doping with Cd and Mg, respectively [3–5]. This further enhances the range of UV detectors for air quality monitoring, gas sensing, military applications, etc [5,6]. Photoresponse characteristics generally depends upon several factors like thickness, grain size, micropores, orientation, doping, annealing and encapsulating layer [7,8]. Several efforts have been directed towards synthesis of nanostructures to control the shape, aspect ratio (length/width), growth site, and growth direction [9,10]. As the growth of ZnO

nanowires by metal organic chemical vapor deposition (MOCVD) is a bottom–up technique, the nature of substrates has a vital role for the determination of nanowire dimension and alignment. However, in the pursuit of next generation ZnO-based nanodevices, it would be highly preferred if well-ordered ZnO nanowires with high aspect ratio could be aligned onto cheap and CMOS compatible substrates, such as silicon. In addition, silicon is the most popular substrate for microelectronics and microelectromechanical systems (MEMS), and it serves as a good integration platform.

Microchannel-based solid-state devices have played an important role for chemical, gas and flow sensors with compact size and superior performance [11–15]. Recently, carbon nanotubes (CNT) based microchannel sensors have also been developed for gas-flow shear stress measurement [16]. For ease of encapsulation, devices in microchannel have an advantage over planar technology [17]. Hence the study of growth and performance of ZnO nanowires in micropatterened substrates is a key issue. In this paper, we report the enhancement of aspect ratio of ZnO nanowires on silicon microchannel. Afterwards, UV response

of the nanowires at the top and bottom surfaces has been studied.

2. Experimental

ZnO nanowires were grown on patterned silicon (p-type, (100), 1–30 Ω cm) substrates using MOCVD system, where diethylzinc (DEZn) was used as the zinc precursor. Before ZnO growth, Si substrates were patterned by wet chemical etching process to form microcavity. At first, 200-nm-thick silicon nitride masking layer was grown by low-pressure chemical vapor deposition (LPCVD) at 800 °C in the mixture of dichlorosilane (SiH$_2$Cl$_2$) and ammonia (NH$_3$) with 240 mTorr pressure. Thereafter, standard photolithography and etching techniques were adopted in order to fabricate micropatterns. Reactive ion etcher (RIE) was used to remove silicon nitride layer from the micro-patterned windows and the etch rate was 350 nm/min. Afterwards, the samples were immersed in KOH solution for 10 h to fabricate the truncated pyramid-shaped etch patterns. Before the growth of ZnO nanowires, no passivation layer was intentionally used. The substrate temperature was kept at 630 °C during the

nanowire growth. The working pressure of the reactor was maintained at 3 Torr and the distance between the susceptor and the nozzle was fixed at 1.5 cm. Morphological investigations of ZnO nanostructures at different position of the microchannel were carried out using field-emission scanning electron microscopy (FESEM, Hitachi S-4200). X-ray diffraction studies were carried out using Rigaku (DMAX-2500 H) system. In addition, the microstructures of ZnO nanowires were observed using high-resolution transmission electron microscopy (HRTEM, JEOL JEM-2100F). The standard shadow-mask technique was used to fabricate the ZnO metal–semiconductor–metal (MSM) UV detectors with Au/Ti electrodes. The designed inter-electrode distance and the photosensitive area were around 1 mm and 0.3 mm^2, respectively. Time-resolved current (at 3 V) was measured with UV (352 nm) exposure using a semiconductor parameter analyzer (HP4145B).

3. Results and discussion

Fig. 1(a) shows the cross sectional image (FESEM) of the microchannel in silicon substrate, which contains ZnO nanowires.
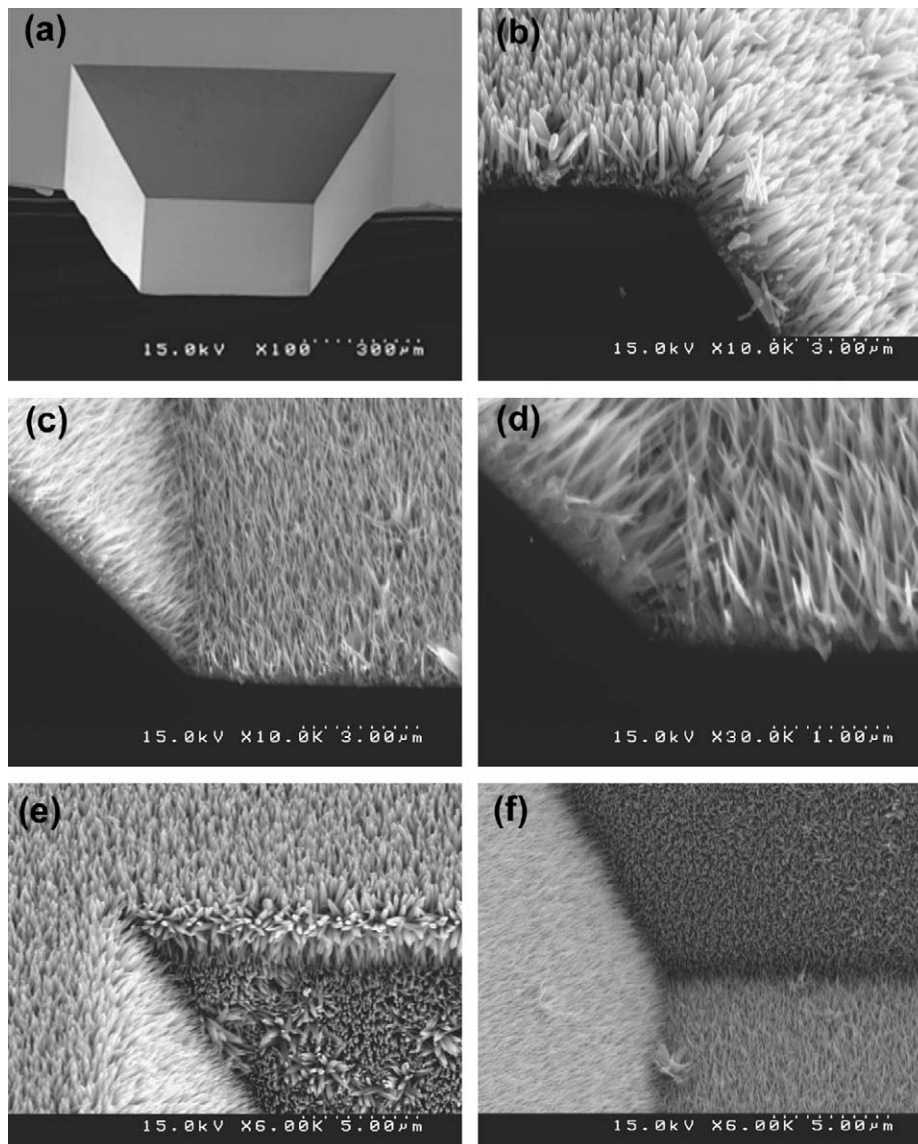
Fig. 1. FESEM images of ZnO nanowires on (a) microchannel, (b) top surface, (c) bottom surface, (d) magnified image of bottom surface, (e) top corner and (f) bottom corner.

Three parts (top surface, side wall and bottom surface) have ZnO nanowires with different dimensions and surface morphologies. On the top of silicon substrate the nanowires were almost uniform along the length (2 μm) and width of 200–250 nm. The aspect ratio, packing fraction and the number density of nanowires on top surface are around 10, 0.8 and 10^7 per mm², respectively. The packing fractions of nanowires were determined by measuring the area occupied by the nanowires on a top view micrograph. Interestingly, vertical nanopencil/tip like ZnO nanostructure was observed towards the bottom of the trench (Fig. 1(c)). Fig. 1(d) depicts that the average basal diameters of the nanopencils are around 100 nm and its shape becomes narrow towards top-end. The nanowires grown towards the bottom of the channel have an aspect ratio, packing fraction and number density of 20, 0.3 and 5×10^7 per mm², respectively. The ZnO nanowires have preferentially grown along a particular direction, which is normal to the substrate surface. It is expected that at the bottom surface the nanowires would have a high perpendicular anisotropy because of the high aspect ratio and the low packing fraction. Figs. 1(e) and (f) show the microstructures of ZnO nanowires at the top and bottom corner of the microchannel, respectively. Furthermore, randomly distributed few nanoflowers are also observed at sidewalls and bottom of the microchannel. It

may be generated from the defects of Si surface, arrived during etching of silicon. The flower has several wings, which have grown from the common origin. These are due to the different directional growth of ZnO nanowires at the defect points. Fig. 2 depicts the XRD pattern of ZnO nanowires grown on Si. Crystalline nature of ZnO nanowires is observed with the appearance of (0 0 0 2) peak. No characteristic diffraction peaks from other phases or impurities were detected. Moreover, the strong intensity of the (0 0 0 2) peak shows that the ZnO nanorods are well oriented along the normal direction of the substrate surface, which is almost consistent with the FESEM observations. This shows that the growth rate of ZnO along c-axis is faster than those of other orientations.

The structural studies of ZnO nanowires grown on Si substrates are reported elsewhere [18]. The bright-field (BF) TEM images of ZnO nanowires in microchannel are shown in Fig. 3(a). In addition to the nanostructures, small irregular fragments are also appeared in the pictures, which might have originated during the removal and/or sonication of nanowires for TEM measurements. Consistent with SEM observations, the ZnO nanowires have the average diameters of 100 nm. In order to further investigate the structural characteristics of ZnO nanowires, high-resolution transmission electron microscopy (HRTEM) experiment was carried out and the magnified image is shown in Fig. 3(b). The HRTEM image indicates that the nanowires are structurally uniform and do not exhibit any noticeable defects. The HRTEM image confirmed that single-crystalline ZnO nanowires are preferentially oriented in the c-axis direction. The spacing of 0.52 nm between adjacent lattice planes also indicates that the preferred growth direction of ZnO single-crystalline nanowires is [0 0 0 1]. The corresponding selected area electron diffraction (SAED) pattern (inset of Fig. 3(b)) projected to the [1 0 0 0] zone axis exhibits visible bright spots corresponding to the crystal planes of the wurtzite structure without any discontinuity and the nanowires possess a single-crystalline hexagonal structure with good crystalline quality along the [0 0 0 1] axis.

The possible growth mechanisms of ZnO nanowires are stated below. At the top surface, high-density island were nucleated on the substrate and grew preferentially along the c-axis orientation. The continuous growth led to the coalescence of these islands and as a result wider nanowires, with a low density and a reduced aspect ratio, were grown [19]. But at the inclined surface, the growth direction (c-axis) and the direction of incoming precursor molecules are not same. So, the width of nanowires is less than
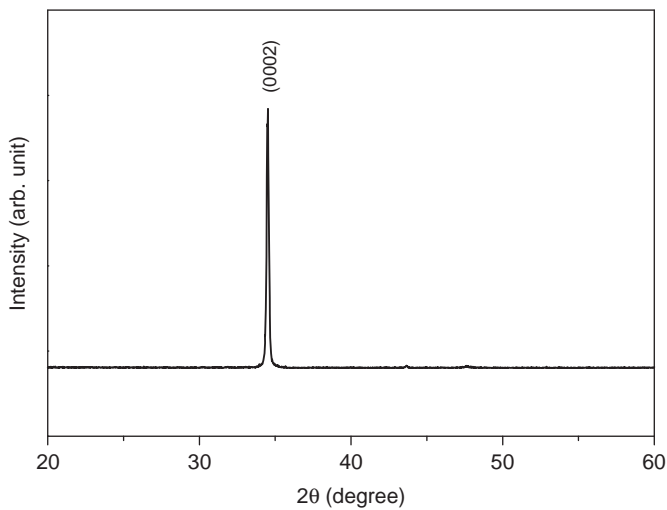
Fig. 2. XRD patterns of ZnO nanostructures grown on Si.
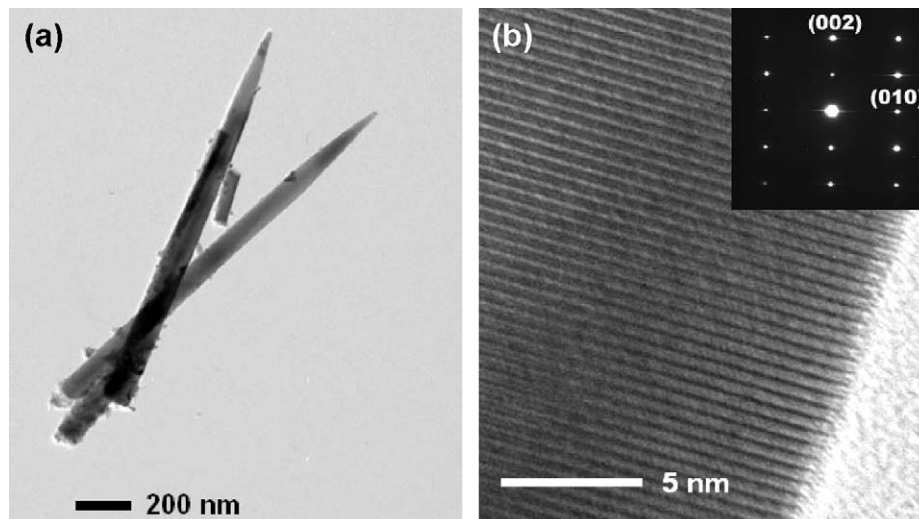
Fig. 3. (a) Bright field image and (b) HRTEM of ZnO nanowires grown on Si microchannel. The inset shows the corresponding SAED pattern from the nanowire.

the top surface. Now at the bottom surface of the microchannel, number of incoming fresh precursor molecule is less than the top surface due to stagnant of gaseous species at the cavity. It is assumed that the sharpness of the tips originates due to the lack of fresh reactant supply to the bottom of cavity during the growth of nanostructures [20]. Thus, the probability of coalescence of grain is less, which leads to the formation of thin nanowires compared to the top surface.

ZnO-nanowires-based UV photodetectors were fabricated on both top and bottom surfaces of the microchannel as shown in Fig. 4(a). The photoresponse behavior (at 3 V) were individually measured for both top and bottom surfaces. Figs. 4(b) and (c) depict the time-resolved UV response of the structures on top and bottom surfaces, respectively. Under UV illumination, the current increased rapidly to a certain level and then gradually became saturated. After turning off, the current tends to come back to its

initial state and this change is exponential. The decay times of the UV detectors fabricated at the bottom and top surfaces were 5 and 100 s, respectively. The higher on/off ratio was also observed for the thin nanowires at the bottom surface.

Initially, a lower base line dark current was observed, which may be due to the trapping of free electrons at the surface of nanowires by the absorption of atmospheric oxygen [21]. These negatively charged surface states introduced a depletion region near the surface, which led to a lower current before UV illumination. When the energy of incident UV light is greater than the bandgap of ZnO nanowires, a large number of electron-hole pairs are created at the surface. The photogenerated holes recombine with the chemisorbed oxygen ions on the surface and eliminate the depletion region. At the same time the electrons contribute to the conduction. After turning off UV light, the surface again absorbs oxygen by reducing free electrons [22]. As a result, the conductance of the nanowires decreases. When the nanowire width decreases, the surface to volume ratio increases. Thus, the absorption and desorption at the surface has greater influence on the conductivity of the sample. Therefore, the higher on/off ratio was obtained at the bottom surface. It has been reported that the photoresponse of UV detectors can be improved by reducing the inter-electrode spacing and surface treatments by polymers [5,23]. The decay of current is also faster for the nanowires grown on the bottom surface of the channel. It is due to the fast recombination of photogenerated electron-hole pairs (solid-state process) and gas reabsorption (surface effects) at the surface [24]. So, the UV detectors, fabricated at the bottom surface of the microchannel, have shown relatively faster response with baseline recovery. Sharma et al. [25] have observed similar results for porous ZnO films. The porous film has larger surface area, which exhibits a fast ultraviolet photoresponse with minimal degradation in comparison to dense film. Furthermore, the photoresponse time depends on the traps centers present in the sensing material. Lower time constant can be achieved by increasing surface to volume ratio [26,27]. In addition, the time constant also depends on both energy and intensity of the illuminated UV lamp [6,8,28]. Law et al. [29] has also observed fast photoresponse due to the surrounding ambient such as presence of water vapors in air.

4. Conclusion

Aligned ZnO nanowires were grown by MOCVD technique on patterned silicon substrate. The shape of ZnO nanostructures was greatly influenced by the patterned substrate surface. The aspect ratio and number density of nanowires increased towards the bottom of the channel, whereas packing fraction decreased. The sharp nanowires were grown at the bottom of the cavity due to the lack of reactant supply during the growth. XRD patterns suggest that the nanowires have good crystallinity. HRTEM image confirmed the single-crystalline growth of the ZnO nanowires along the [0 0 0 1] direction. Photosensitivity for the nanowires, grown on both top and bottom surface of the microchannel, was measured. The higher current on/off ratio with faster decay was observed for the nanowires grown on the bottom surface.

Acknowledgements
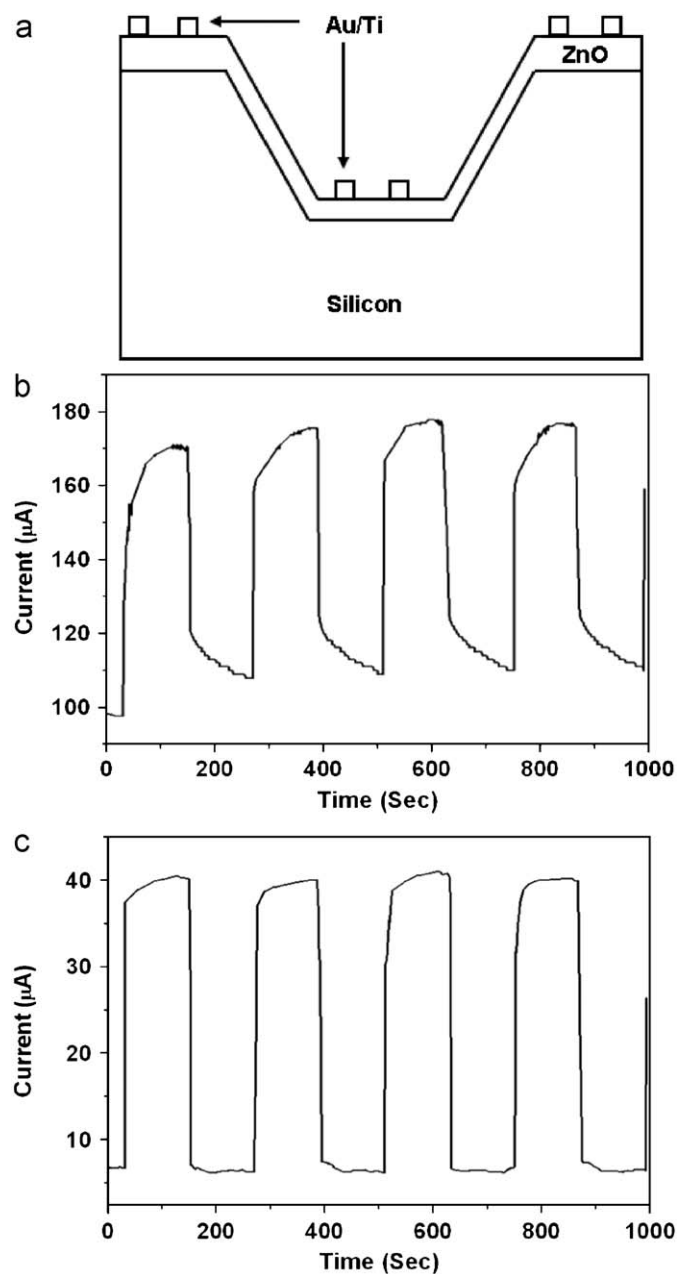
Fig. 4. (a) Schematic lay out of UV detectors and time-resolved photoresponse of the structures on (b) top surface and (c) bottom surface of microchannel.

References

[1] J.G. Lu, P. Chang, Z. Fan, Mater. Sci. Eng. R 52 (2006) 49.

[2] C.H. Liu, W.C. Yiu, F.C.K. Au, J.X. Ding, C.S. Lee, S.T. Lee, Appl. Phys. Lett. 83 (2003) 3168.

[3] Y. Liu, C.R. Gorla, S. Liang, N. Emanetoglu, Y. Lu, H. Shen, M. Wraback, J. Electron. Mater. 29 (1) (2000) 69.

[4] S.J. Pearton, W.T. Lim, J.S. Wright, L.C. Tien, H.S. Kim, D.P. Norton, H.T. Wang, B.S. Kang, F. Ren, J. Jun, J. Lin, A. Osinsky, J. Electron. Mater. 37 (9) (2008) 1426.

[5] S.S. Hullavarad, N.V. Hullavarad, P.C. Karulkar, A. Luykx, P. Valdivia, Nanoscale Res. Lett. 2 (2007) 161.

[6] X.G. Zheng, Q.S. Li, Cent. Eur. J. Phys. 6 (2) (2008) 351.

[7] R. Ghosh, B. Mallik, D. Basak, Appl. Phys. A 81 (2005) 1281.

[8] C.Y. Liu, B.P. Zhang, Z.W. Lu, N.T. Binh, K. Wakatsuki, Y. Segawa, R. Mu, J. Mater. Sci: Mater. Electron. 20 (2009) 197.

[9] Y. Sun, N.G. Ndifor-Angwafor, D.J. Riley, M.N.R. Ashfold, Chem. Phys. Lett. 431 (2006) 352.

[10] S.W. Lee, M.C. Jeong, J.M. Myoung, G.S. Chae, I.J. Chung, Appl. Phys. Lett. 90 (2007) 133115-1.

[11] Y.S. Kim, S.C. Ha, K. Kim, H. Yang, S.Y. Choi, Y.T. Kim, J.T. Park, C.H. Lee, J. Choi, J. Paek, K. Lee, Appl. Phys. Lett. 86 (2005) 213105.

[12] A. Rasmussen, M. Gaitan, L.E. Locascio, M.E. Zaghloul, J. Microelectromech. Syst. 10 (2001) 286.

[13] J.B. Sanchez, F. Berger, M. Fromm, M.H. Nadal, Sensors Actuators B 119 (2006) 227.

[14] B. Yu, Z. Gan, S. Cao, J. Xu, S. Liu, 11th Intersociety Conference on Thermal and Thermomechanical Phenomena in Electronic Systems (ITHERM) 28–31 May (2008) 215.

[15] Y. Sekimori, Y. Yoshida, T. Kitamori, in: Proceedings of IEEE Sensors 24–27 October (2004) 1516.

[16] W.W.Y. Chow, W.J. Li, S.C.H. Tung, Proceedings of the 3rd IEEE International Conference on Nano/Micro Engineered and Molecular Systems 6–9 January (2008) 1011.

[17] P. Pal, S. Chandra, Smart Mater. Struct. 13 (2004) 1424.

[18] J.P. Kar, S.W. Lee, W. Lee, J.M. Myoung, Appl. Surf. Sci. 254 (2008) 6677.

[19] D.J. Park, J.Y. Lee, D.C. Kim, S.K. Mohanta, H.K. Cho, Appl. Phys. Lett. 91 (2007) 143115.

[20] S. Lee, A. Umar, S.H. Kim, N.K. Reddy, Y.B. Hahn, Korean J. Chem. Eng. 24 (2007) 1084.

[21] O. Lupan, L. Chow, G. Chai, L. Chernyak, O.L. Tirpak, H. Heinrich, Phys. Stat. Sol. (a) 205 (11) (2008) 2673.

[22] Z. Bi, J. Zhang, X. Bian, D. Wang, X.A. Zhang, W. Zhang, X. Hou, J. Electron. Mater. 37 (5) (2008) 760.

[23] C.S. Lao, M.C. Park, Q. Kuang, Y. Deng, A.K. Sood, D.L. Polla, Z.L. Wang, J. Am. Chem. Soc. 129 (2007) 12096.

[24] Y. Li, F.D. Valle, M. Simonnet, I. Yamada, J.J. Delaunay, Nanotechnology 20 (2009) 045501.

[25] P. Sharma, A. Mansingh, K. Sreenivas, Appl. Phys. Lett. 80 (4) (2002) 553.

[26] Y.W. Heo, B.S. Kang, L.C. Tien, D.P. Norton, F. Ren, J.R. La Roche, S.J. Pearton, Appl. Phys. A 80 (2005) 497.

[27] A. Bera, D. Basak, Appl. Phys. Lett. 93 (2008) 053102.

[28] G. Cherkashinin, V. Lebedev, R. Wagner, I. Cimalla, O. Ambacher, Phys. Stat. Sol. (b) 243 (7) (2006) 1713.

[29] J.B.K. Law, J.T.L. Thong, Appl. Phys. Lett. 88 (2006) 133114.